UCL-IPT-05-18, CPHT-RR-008.0106

CP asymmetry and branching ratio of $B \to \pi\pi$

E. Kou[1*] and T. N. Pham[2†]
[1] *Institut de Physique Théorique, Université Catholique de Louvain, B1348, Belgium*
[2] *Centre de Physique Théorique, Centre National de la Recherche Scientifique, UMR 7644 Ecole Polytechnique, 91128 Palaiseau, Cedex, France*

(Dated: December 22, 2013)

We investigate the branching ratios and CP asymmetries of the $B \to \pi\pi$ processes measured in B factory experiments. Fits to the experimental data of this process indicate a large ratio of color-suppressed (C) to color-allowed (T) tree contributions. We investigate whether the large C/T can be explained within the QCD based model computation with i) a large effect from the end-point singularity or with ii) large final-state-interaction phase between two different isospin amplitudes. We show that the current experimental data do not exclude either possibility but we may be able to distinguish these two effects in future measurements of direct CP asymmetry of $B^0 \to \pi^0\pi^0$.

PACS numbers: 13.20.He

I. INTRODUCTION

Recent measurements of the branching ratio and CP asymmetry of the $B \to \pi\pi$ process provide us with a deep insight into the nature of both weak and strong interactions. The measurement of the direct CP asymmetry in $B^0 \to \pi^+\pi^-$ clearly indicate that there is a substantial contribution from the $b \to d$ penguin-loop diagram in addition to the dominant $b \to u$ tree-level diagram, which considerably complicates the extraction of the weak phase $\alpha(\phi_2)$ from this process. Furthermore, new physics contributions to this penguin diagram are not yet excluded. Although the $B_d - \overline{B}_d$ oscillation measurement constrains very strictly the new physics contribution to the $b \to d$ transition coming from the box diagram, the one-loop penguin diagrams could still get additional contributions in various new physics models (see [1] for an example). On the other hand, the biggest challenge in the analysis of the $B \to \pi\pi$ processes lies in the difficulty of estimating the relative sizes of different topologies, which are governed not only by weak interactions but also by strong interactions. Therefore, an understanding of the strong interaction effects in these processes is crucial for extracting the weak phase and ultimately, possible new physics contributions.

Recently, the combined analysis of the CP asymmetries of $B^0 \to \pi^+\pi^-$ and the branching ratios of $B^0 \to \pi^+\pi^-$, $B^0 \to \pi^0\pi^0$ and $B^0 \to \pi^+\pi^0$ showed interesting results for the relative sizes of different types of the tree diagrams. At the leading order in QCD, the ratio of the color-suppressed to the color-allowed tree diagram, which we call C/T, is $1/N_c$, where N_c is the number of colour, i.e $N_c = 3$ in QCD. On the contrary, various model-independent analysis of experimental data indicates however C/T is close to unity [2]-[16]. We here would like to investigate whether this large value of C/T can be explained by higher order QCD corrections or other hadron dynamics.

In this article, we investigate two possible enhancement factors of C/T, i) the higher order correction of the QCD based model (QCD factorization) [17], [18] and ii) the effect of FSI phase. For i), we present an anatomy of the higher order QCD corrections and discuss in detail, the effect of the free parameters using the c-convention [2]. We also show that C/T in QCD factorization, in the c-convention which we use in this analysis, contains contributions from top- and up-penguin as well as annihilation diagrams in addition to the pure color-suppressed tree diagrams. According to QCD factorization, these annihilation terms which suffer from the end-point singularity and contain free parameters could play an important role in the enhancement of the C/T ratio. Estimate of annihilation contributions in QCD sum-rule can be found in [19]. For ii), it was found in [20] that C/T can be *effectively* enhanced by including non-zero FSI phase. We examine this possibility in detail. In this analysis, we use a "bare" C/T ratio estimated from QCD factorization but by suppressing the strong phase from the perturbative computation. The other approach including both perturbative and FSI phases can be found in [22].

The remaining of the article is organised as follows. In section II, we fit the experimental data to a model independent parameterization. In section III, we show the prediction of QCD factorization for the parameters defined in section II. In section IV, we introduce the FSI phase based on the isospin decomposition of the amplitude and show how large $(C/T)_{\text{eff}}$ can get to. And finally, we conclude in section V.

II. MODEL INDEPENDENT FIT OF EXPERIMENTAL DATA

In this section, we first introduce a model independent parameterization for the amplitudes of the $B \to \pi\pi$ processes and summarize the fitted values of these parameters to the experimental data. Let us start by giving

*email address: ekou@fyma.ucl.ac.be
†email address: Tri-Nang.Pham@cpht.polytechnique.fr

γ / $(S_{\pi^+\pi^-}, C_{\pi^+\pi^-})$	27°	37°	47°	57°	67°	77°	87°
(-0.62, -0.47)	0.53 −155° 0.43	0.38 −131° 0.75	0.36 −92.6° 1.10	0.46 −61.7° 1.45	0.63 −45.0° 1.75	0.81 −35.5° 1.96	0.98 −29.5° 2.06
(-0.62, -0.27)	0.49 −166° 0.40	0.29 −147° 0.69	0.19 −92.1° 1.03	0.32 −43.4° 1.35	0.52 −27.5° 1.63	0.72 −20.5° 1.82	0.91 −16.6° 1.91
(-0.50, -0.37)	0.55 −164° 0.35	0.38 −149° 0.62	0.26 −115° 0.92	0.29 −66.6° 1.21	0.44 −41.3° 1.46	0.62 −29.8° 1.63	0.80 −23.4° 1.72
(-0.38, -0.47)	0.61 −164° 0.33	0.45 −150° 0.58	0.33 −125° 0.85	0.31 −86.9° 1.12	0.41 −56.7° 1.35	0.56 −40.4° 1.51	0.72 −31.2° 1.58
(-0.38, -0.27)	0.59 −170° 0.31	0.40 −162° 0.55	0.23 −140° 0.81	0.17 −79.1° 1.07	0.31 −37.8° 1.28	0.49 −24.1° 1.44	0.67 −17.8° 1.51

TABLE I: Determination of P/T (upper value), δ_{PT} (middle value) and R (lower value) using experimental results for $S_{\pi^+\pi^-} = (-0.50 \pm 0.12)$ and $C_{\pi^+\pi^-} = (-0.37 \pm 0.10)$ for given values of γ, $\gamma = (27^\circ \sim 87^\circ)$.

the amplitudes of the $B \to \pi\pi$ processes in terms of T (color-allowed tree), C (color-suppressed tree), P (penguin), which correspond to different topologies, which we discuss later on:

$$\begin{aligned}
\mathrm{Amp}(B^0 \to \pi^+\pi^-) &= Te^{i\delta_t}e^{i\gamma} + Pe^{i\delta_P} && (1)\\
\sqrt{2}\mathrm{Amp}(B^0 \to \pi^0\pi^0) &= Ce^{i\delta_C}e^{i\gamma} - Pe^{i\delta_P} && (2)\\
\sqrt{2}\mathrm{Amp}(B^+ \to \pi^+\pi^0) &= (Te^{i\delta_T} + Ce^{i\delta_C})e^{i\gamma}, && (3)
\end{aligned}$$

where δ_i's is the strong phase and γ is the CP violating phase. In the following, we analyse 5 observables of the $B \to \pi\pi$ process, which are experimentally found to be [23]

$$\begin{aligned}
S_{\pi^+\pi^-} &= -0.50 \pm 0.12 && (4)\\
C_{\pi^+\pi^-} &= -0.37 \pm 0.10 && (5)\\
\mathrm{Br}(\pi^+\pi^-) &= (4.5 \pm 0.4) \times 10^{-6} && (6)\\
\mathrm{Br}(\pi^0\pi^0) &= (1.45 \pm 0.29) \times 10^{-6} && (7)\\
\mathrm{Br}(\pi^+\pi^0) &= (5.5 \pm 0.6) \times 10^{-6} && (8)
\end{aligned}$$

where $\mathrm{Br}(f_1 f_2)$ represents the CP-averaged branching ratios, $\mathrm{Br}(f_1 f_2) = (Br(B \to f_1 f_2) + Br(\bar{B} \to \bar{f}_1 \bar{f}_2))/2$. The time-dependent CP asymmetry of $B \to \pi^+\pi^-$ is defined as

$$\begin{aligned}
A_{\pi^+\pi^-}(t) &= \frac{\Gamma_{\bar{B}(t)\to\pi\pi} - \Gamma_{B(t)\to\pi\pi}}{\Gamma_{\bar{B}(t)\to\pi\pi} + \Gamma_{B(t)\to\pi\pi}} && (9)\\
&= S_{\pi^+\pi^-}\sin(\Delta M_B t) - C_{\pi^+\pi^-}\cos(\Delta M_B t)
\end{aligned}$$

where

$$S_{\pi^+\pi^-} = \frac{2Im\left(\frac{q}{p}\bar{\rho}_{\pi^+\pi^-}\right)}{1+|\bar{\rho}_{\pi^+\pi^-}|^2}, \quad C_{\pi^+\pi^-} = \frac{1-|\bar{\rho}_{\pi^+\pi^-}|^2}{1+|\bar{\rho}_{\pi^+\pi^-}|^2} \qquad (10)$$

with $\bar{\rho} = \mathrm{Amp}(\overline{B}^0 \to \pi^+\pi^-)/\mathrm{Amp}(B^0 \to \pi^+\pi^-)$ and $|B_{1,2}\rangle = p|B^0\rangle \pm q|\overline{B}^0\rangle$. In the standard model, we have $\frac{q}{p} = \frac{V_{tb}^* V_{td}}{V_{tb} V_{td}^*} = e^{-2i\beta}$ and $\beta(\phi_1)$ is measured in a very high precision from the time-dependent CP asymmetry of $B \to J/\psi K_S$. Using Eq. (1), we obtain

$$\bar{\rho}(\pi^+\pi^-) = \frac{Te^{i\delta_T}e^{-i\gamma} + Pe^{i\delta_P}}{Te^{i\delta_T}e^{i\gamma} + Pe^{i\delta_P}} \qquad (11)$$

and then, using $\alpha+\beta+\gamma = \pi$, we find (find more detailed derivation, e.g. in [2]),

$$\begin{aligned}
&R\ S_{\pi^+\pi^-} && (12)\\
&= \sin 2\alpha + 2\sin(\beta-\alpha)\cos\delta_{PT}\left(\frac{P}{T}\right) - \sin 2\beta\left(\frac{P}{T}\right)^2\\
&R\ C_{\pi^+\pi^-} && (13)\\
&= 2\sin(\alpha+\beta)\sin\delta_{PT}\left(\frac{P}{T}\right)
\end{aligned}$$

where

$$R = 1 - 2\cos(\alpha+\beta)\cos\delta_{PT}\left(\frac{P}{T}\right) + \left(\frac{P}{T}\right)^2. \qquad (14)$$

As for the branching ratios, we follow [24] and use the ratios of the averaged branching ratios, which are derived from Eq. (1), Eqs. (2) and (3) as

$$\begin{aligned}
R_{00} &= \frac{2\mathrm{Br}(\pi^0\pi^0)}{\mathrm{Br}(\pi^+\pi^-)} && (15)\\
&= \frac{1}{R}\left[\left(\frac{C}{T}\right)^2 + \left(\frac{P}{T}\right)^2\right.\\
&\quad \left. -2\cos(\delta_{PT}-\delta_{CT})\cos\gamma\left(\frac{C}{T}\right)\left(\frac{P}{T}\right)\right]\\
R_{+-} &= \frac{2\mathrm{Br}(\pi^+\pi^0)\tau_{B^0}}{\mathrm{Br}(\pi^+\pi^-)\tau_{B^+}} && (16)\\
&= \frac{1}{R}\left[1 + 2\cos\delta_{CT}\left(\frac{C}{T}\right) + \left(\frac{C}{T}\right)^2\right]
\end{aligned}$$

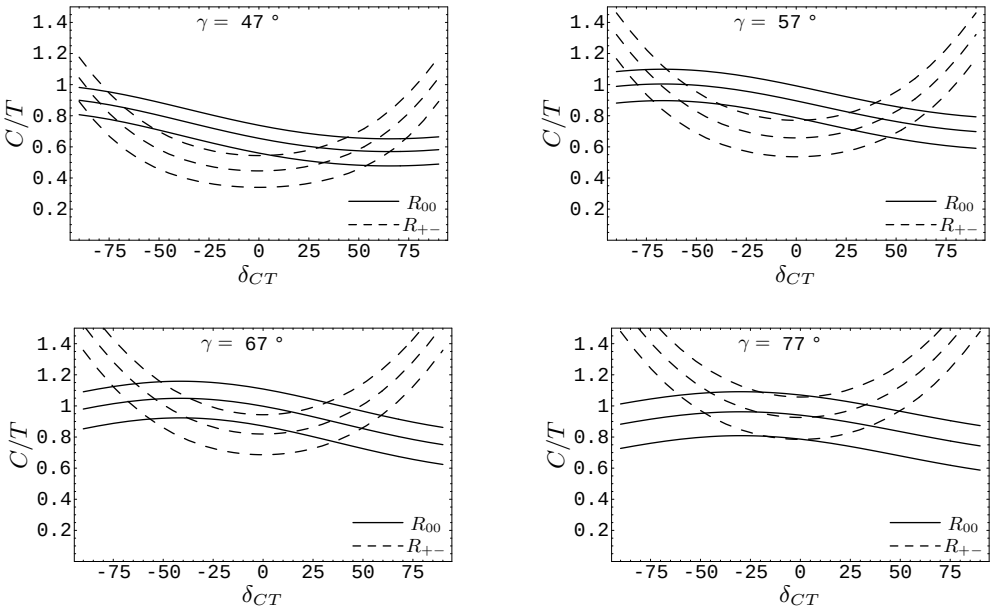

FIG. 1: Allowed region for δ_{CT} (x-axis) versus C/T (y-axis), obtained from experimental bounds for R_{00} and R_{+-}. The numerical results for P/T and δ_{PT} obtained from the central value of the asymmetry measurements, $(S_{\pi^+\pi^-}, C_{\pi^+\pi^-}) = (-0.50, -0.37)$ (see Table 1) are used. The three solid lines represent $R_{00} = 0.64 - 0.14,\ 0.64,\ 0.64 + 0.14$, and the three dashed lines represent $R_{+-} = 2.27 - 0.32,\ 2.27,\ 2.27 - 0.32$. The overlap of solid and dashed bounds are the allowed region for C/T and δ_{CT}. The weak phase γ is fixed as left-top ($\gamma = 47^\circ$), right-top ($\gamma = 57^\circ$), left-bottom ($\gamma = 67^\circ$), right-bottom ($\gamma = 77^\circ$).

where $\delta_{ab} \equiv \delta_a - \delta_b$.

Before discussing our result, we would like to make a comment on the direct CP asymmetry of the $\pi^0\pi^0$ channel, C_{00}. In the same parameterization, one can write:

$$C_{00} = \frac{2\sin\gamma\sin(\delta_{CT} - \delta_{PT})\left(\frac{C}{T}\right)\left(\frac{P}{T}\right)}{\left(\frac{C}{T}\right)^2 + \left(\frac{P}{T}\right)^2 - 2\cos\gamma\cos(\delta_{CT} - \delta_{PT})\left(\frac{C}{T}\right)}. \quad (17)$$

The experimental bound is given as [23]:

$$C_{00} = 0.28^{+0.40}_{-0.39}. \quad (18)$$

Since the experimental data is not very precise yet, we will not include this data in our analysis but will discuss its relevance to the strong phase δ_{CT} in subsequent sections.

Now using these formulae, we shall fit the parameters to the experimental data. Table 1 shows determinations of P/T (upper values) , δ_{PT} (middle values) and R (bottom values) by using experimental values of $S_{\pi^+\pi^-}$ and $C_{\pi^+\pi^-}$ for given values of γ, by using $\beta = 23.7^\circ$. We can find that the R value becomes larger than unity in the most of the parameter space for $\gamma > 57^\circ$. We also find that R is particularly larger when $S_{\pi^+\pi^-}$ is larger and negative.

Next inputting the values of P/T and δ_{PT} obtained from the above analysis into the R.H.S. of Eq. (15) and Eq. (16) and the experimental values of R_{00} and R_{+-} into the L.H.S., we compute C/T and δ_{CT}. We first use only the central value of $(S_{\pi^+\pi^-}, C_{\pi^+\pi^-}) = (-0.50, -0.37)$ but include 1σ experimental error for R_{00} and R_{+-}. Obtained results for $\gamma = 47^\circ$ (left-top), 57° (right-top), 67° (left-bottom), 77° (right-bottom) are shown in Fig. 1. The overlap of the solid (R_{00}) and the dashed (R_{+-}) bounds shift towards the larger C/T region as γ becomes larger, or equivalently R becomes larger. Therefore, the large value of R, which is originated from the large negative $S_{\pi^+\pi^-}$, causes the large value of C/T. Furthermore, we find that R_{+-} allows relatively small value of C/T while R_{00} leads to a more strict constraint, $C/T \gtrsim 0.5$. We find that the overlap region is distributed in a large range of δ_{CT}. Let us now discuss the errors coming from $(S_{\pi^+\pi^-}, C_{\pi^+\pi^-})$, since Fig. 1 is obtained by using only their central values. First, both R_{00} and R_{+-} depend on $(S_{\pi^+\pi^-}, C_{\pi^+\pi^-})$ through R, as $1/R$ as mentioned above. While R_{+-} does not have further P/T and δ_{pt} dependence, R_{00} has more complex dependence on them. However, as long as the overlap region is concerned, we find that the derived error is up to $\pm$ a few % in C/T and $\pm 20^\circ$ in δ_{CT}.

From the above analysis, we can not obtain a strong constraint on the weak phase γ. While measurements for e.g. the direct CP asymmetry of the $\pi^0\pi^0$ channel would allow a determination of γ in the future, currently, we need some inputs from theoretical models. Especially, the value of C/T found from the fits in this section seems to be rather large comparing to the leading order prediction. Therefore, we will try to extract bounds for C/T and δ_{CT} using the theoretical models in the following section, which in turn may give us a constraint on γ.

III. QCD MODEL CALCULATION OF PARAMETERS C, T AND P

In this section, we investigate whether those fitted values on C/T and δ_{CT} can be reproduced by the QCD factorization. Let us first give the relation between the parameterisation of the amplitudes in Eqs. (1) to (3) in the previous section and the one in QCD factorization:

$$Te^{i\delta_T}e^{\gamma} \propto \lambda_u^*(a_1+b_1+\hat{a}_4^u), \quad (19)$$
$$Ce^{i\delta_C}e^{\gamma} \propto \lambda_u^*(a_2-b_1-\hat{a}_4^u), \quad (20)$$
$$Pe^{i\delta_P} \propto \lambda_c^*\hat{a}_4^c \quad (21)$$

where

$$\hat{a}_4^p = a_4^p + r_\chi a_6^p + 2b_4 + b_3 \quad (22)$$

and $r_\chi = 2m_\pi^2/(2m_b m_q) \simeq 1.24$ with $m_q \equiv (m_u+m_d)/2$. Here we employ the so-called c-convention, which eliminates λ_t by using an unitarity relation. Therefore, the amplitudes are proportional only to two CKM factors λ_u and λ_c

$$\lambda_u = V_{ub}V_{ud}^* \simeq A\lambda^3(\rho - i\eta) \quad (23)$$
$$\lambda_c = V_{cb}V_{cd}^* = \simeq -A\lambda^3. \quad (24)$$

Note that $\arg(\rho - i\eta) = e^{i\gamma}$ and $|\rho - i\eta| = |\lambda_u^*/\lambda_c^*|$. It is important to notice that apart from the "pure" color-allowed tree contribution a_1 and the "pure" color-suppressed tree contribution a_2, $Te^{i\delta_T}$ and $Ce^{i\delta_C}$ contain the same two terms with opposite sign, which are penguin- and tree-annihilations contributions (b_i terms) and top- and up-penguin contributions (a_4^u). As has already been investigated in [18], it is quite possible that these contributions could effectively enhance the ratio C/T by contributing constructively and destructively to C and T, respectively. In this respect, the sign of these extra contributions must be carefully investigated.

In order to understand the size of the higher order corrections estimated by the QCD factorization, we first give an expression decomposing a_i^p and b_i into factorisable terms and their correction terms:

$$a_i^p = \left(C_i + \frac{C_{i\pm1}}{N_c}\right) + \frac{C_{i\pm1}}{N_c}\frac{C_F\alpha_s}{i\pi}\left[V_i + \frac{4\pi^2}{N_c}H_i\right] + P_i^p \quad (25)$$

$$b_1 = \frac{C_F}{N_c^2}C_1A_1^i \quad (26)$$

$$b_3 = \frac{C_F}{N_c^2}[C_3A_1^i + C_5(A_3^i + A_3^f) + N_cC_6A_3^f] \quad (27)$$

$$b_4 = \frac{C_F}{N_c^2}[C_4A_1^i + C_6A_2^i] \quad (28)$$

where $p = u, c$. The sign $\pm$ in a_i must be taken as $+$ for $i =$ odd and $-$ for $i =$ even. The first terms of a_i^p are called factorisable term. The term proportional to $V_i, H_i, P_i^p, A_i^{i,f}$ are the vertex correction, hard-scattering correction, penguin correction and annihilation correction, respectively. At the leading order, all the Wilson coefficients vanish except C_1 with $C_1 = 1$, which leads to

$$C/T = 1/3, \qquad P/T = 0, \qquad \text{At LO.} \quad (29)$$

The numerical results including all the above higher order corrections are shown in Table 2. For the input parameters, we use the central values in the Table 1 of [18], among which we list some important ones here;

$$\mu = 4.2\text{GeV}, \quad m_q(2\text{GeV}) = 0.0037\text{GeV}, \quad \lambda_B = 0.35\text{GeV}, \quad |\lambda_u/\lambda_c| = |\rho + i\eta| = 0.09, \quad \alpha_2^\pi = 0.1 \quad (30)$$

where λ_B and α_2^π are the parameters for the distribution amplitude of B meson and π, respectively (for theoretical estimates of these parameters, see e.g. [25]-[27] and [28]). The value of m_q must be running to the appropriate scales in the computation. The numbers in the parenthesis in Table 2 are the results with a smaller renormalisation scale, $\mu = 2.1$ GeV (the other parameters are the same as before). We can see that the Wilson coefficients C_{2-6} are $O(\alpha_s)$ suppressed comparing to C_1 and a_1 is completely dominated by the factorisable term. On the other hand, the factorisable term of a_2 is rather small since C_2 is $O(\alpha_s)-$ suppressed and there is a color factor $1/N_c$ in C_1 term and furthermore, these two have opposite signs. As a result, the higher order corrections, V_2 and H_2 terms, which are proportional to the leading order Wilson coefficient C_1, lead to large contributions in a_2. It is also important to notice that these correction terms can induce a large strong phase in a_2 which has a comparable real and imaginary part in contrast to a_1 which is almost real. In fact, in the soft-colliner effective theory (SCET) [29] -[31], this correction to a_2 which is proportional to a large coefficient C_1 contains some free parameters. So it could be much more enhanced in SCET; as much as solving the problem of large C/T. A more recent analysis in SCET can also be found in [32]. The smaller μ value reduces the factorisable term of a_2 and thus, the C/T value. We should also mention that the penguin terms $a_{4(6)}^u$ and $a_{4(6)}^c$ are quite similar apart from penguin correction terms. The difference in the penguin corrections is due to charm- and up-penguin difference. Using the results with the default renormalisation scale, $\mu = 4.2$ GeV, we find

$$a_1 = 1.02e^{i0.8^\circ} - 0.014\rho_H e^{i\phi_H} \quad (31)$$
$$a_2 = 0.21e^{-i23^\circ} + 0.081\rho_H e^{i\phi_H} \quad (32)$$
$$a_4^u + r_\chi a_6^u = -0.097e^{i21^\circ} + 0.0010\rho_H e^{i\phi_H} \quad (33)$$
$$a_4^c + r_\chi a_6^c = -0.10e^{i7^\circ} + 0.0010\rho_H e^{i\phi_H} \quad (34)$$

and

$$b_1 = 0.027 + 0.063\rho_A e^{i\phi_A} + 0.0085(\rho_A e^{i\phi_A})^2 \quad (35)$$
$$b_3 = -0.0067 - 0.021\rho_A e^{i\phi_A} - 0.015(\rho_A e^{i\phi_A})^2 \quad (36)$$
$$b_4 = -0.0019 - 0.0046\rho_A e^{i\phi_A} - 0.00061(\rho_A e^{i\phi_A})^2. \quad (37)$$

	factorisable	vertex corr.	hart-scat. corr.	penguin corr.
a_1	1.02 (1.04)	$0.032e^{i27^\circ}(0.044e^{i42^\circ})$	$-0.032-0.014\rho_H e^{i\phi_H}(-0.061-0.025\rho_H e^{i\phi_H})$	0 (0)
a_2	0.17(0.085)	$-0.18e^{i27^\circ}(-0.19e^{i42^\circ})$	$0.18+0.081\rho_H e^{i\phi_H}(0.24+0.095\rho_H e^{i\phi_H})$	0 (0)
a_4^u	$-0.031(-0.046)$	$-0.0023e^{i27^\circ}(-0.0034e^{i42^\circ})$	$0.0023+0.0010\rho_H e^{i\phi_H}(0.0047+0.0019\rho_H e^{i\phi_H})$	$0.014e^{-i73^\circ}(0.022e^{-i50^\circ})$
a_4^c	$-0.031(-0.046)$	$-0.0023e^{i27^\circ}(-0.0034e^{i42^\circ})$	$0.0023+0.0010\rho_H e^{i\phi_H}(0.0047+0.0019\rho_H e^{i\phi_H})$	$-0.0047e^{i76^\circ}(0.0084e^{-i27^\circ})$
a_6^u	$-0.039(-0.060)$	$-0.00047(-0.00083)$	0(0)	$-0.014e^{i79^\circ}(0.017e^{-i73^\circ})$
a_6^c	$-0.039(-0.060)$	$-0.00047(-0.00083)$	0(0)	$-0.0073e^{i38^\circ}(0.0038e^{-i78^\circ})$

TABLE II: Anatomy of the higher order correction in the QCD factorization. For the input paramters, we use the central values given in [18]. The numbers in the parenthesis are obtained by changing renormalisation scale to $\mu = 2.1$ GeV from the default value.

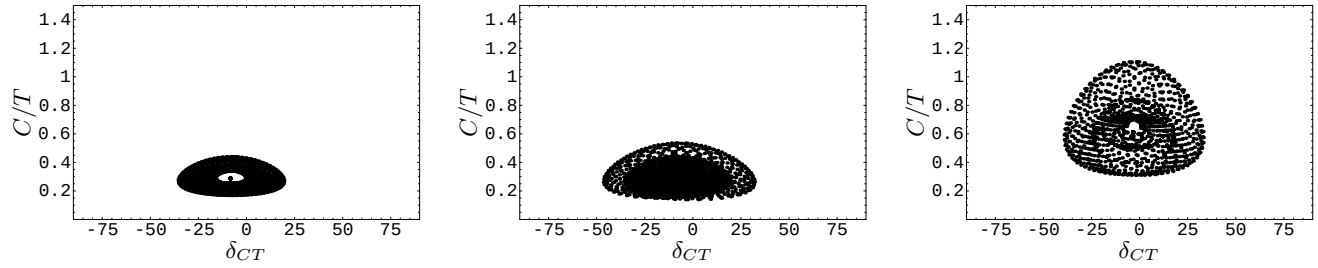

FIG. 2: Scattered plot of the QCD factorization estimate for δ_{CT} (x-axis) versus C/T (y-axis) including the end-point singularity effects. In the plot, we fix the ρ parameters as $(\rho_H, \rho_A) = (1, 1)$ (left) and $= (1, 2)$ (middle) and vary the phases in the range of $-\pi < \phi_{A,H} < \pi$ (interval of 0.2 radian). The rest of the parameters are fixed (see text for details). The last figure (right) is obtained in the same manner with $(\rho_H, \rho_A) = (1, 1)$ but with different parameter set, the so-called scenario 2 of QCD factorization (see text for details).

The parameters $\rho_{A,H}$ and $\phi_{A,H}$ which originate from the end-point singularity would vary, say, in the ranges of $|\rho_{A,H}| < 1 \sim 2$ and $-\pi < \phi_{A,H} < \pi$. We find that ρ_H and ϕ_H have significant contributions to a_2, i.e. C and ρ_A and ϕ_A to b_i, i.e. all of T, C, P. According to Eqs. (19) and (20), in the $c-$ convention, C/T is not simply a_2/a_1 but includes extra contributions from $\hat{a}_4^u$ and b_1, which, we find, are as large as a_2 and strongly depend on ρ_A and ϕ_A. We perform complete analysis of C/T covering all the parameter space of ρ's and ϕ's next. Here, however, it is very important to notice that at the limit of $\rho_{H,A} = 0$, numerical values of $a_{1,2}$ and $a_{4,6}^u$ have the opposite sign, which enhances C and suppress T (see Eqs. (19) and (20)), i.e. the inclusion of $a_{4,6}^u$ terms increases C/T. As a result, we obtain:

$$\frac{C_0}{T_0} e^{i\delta_{CT_0}} = 0.29 e^{-i8.5\circ} \tag{38}$$

where the index 0 indicates $\rho_{H,A} = 0$. We emphasize once more that the signs of $a_{4,6}^u$ and $a_{4,6}^c$ must be the same unless there is large enhancement factors for $c-$ and/or $u-$penguins. And most importantly, the sign of $a_{4,6}^c$ can be fixed from determinations of P and δ_{PT} up to well-known λ_c factor (see, Eq. (21)).

Next we consider the effect of the end-point singularity, $\rho_{H,A}$ and $\phi_{H,A}$, which often cause large theoretical uncertainties in the prediction of QCD factorization. The behaviour of C/T when varying freely these four parameters is rather complicated. In Fig. 2, we show scattered plots of δ_{CT} (x-axis) versus C/T (y-axis) varying the parameters in the range of $-\pi < \phi_{A,H} < \pi$ (interval of 0.2 radian) and fixing $\rho_H = 1$ (left; $\rho_A = 1$, middle; $\rho_A = 2$). We can see that quite a large range of C/T and δ_{CT} are allowed from QCD factorization, C/T up to 0.45 (0.55) for $\rho_A = 1(2)$. In particular, the value of C/T becomes large at small negative values of δ_{CT}. For the case of $\rho_A = 1$ and $\rho_A = 2$, we obtain a constraint respectively, $\gamma \leq 44^\circ(52^\circ)$ and $\gamma \leq 46^\circ$ (56°) allowing $1\sigma(2\sigma)$ error in the experimental values, $S_{\pi^+\pi^-}, C_{\pi^+\pi^-}, R_{00}, R_{+-}$.

In the original paper of QCD factorization [18], the problem of the small a_2 value has already been recognized and a possible solution was proposed, choosing the largest value of the Gegenbauer moment of π distribution amplitude, $\alpha_2^\pi \simeq 0.4$ and the smallest value of the first negative moment of the B meson distribution function, $\lambda_B = 0.2$ GeV (scenario 2). More recently, this approximation has been reanalysed by using QCD factorization with the 1-loop (NNLO) corrections to hard spectator-scattering diagram [33]. In this way, the hard-scattering correction is enhanced by a factor of two, which leads to

$$a_2 \simeq 0.48 e^{-i10^\circ} + 0.18\rho_H e^{i\phi_H} \tag{39}$$

We found that the effect to a_1 is small since a_1 is dominated by the leading order contribution which does not depend on those parameters. As a result, we obtain

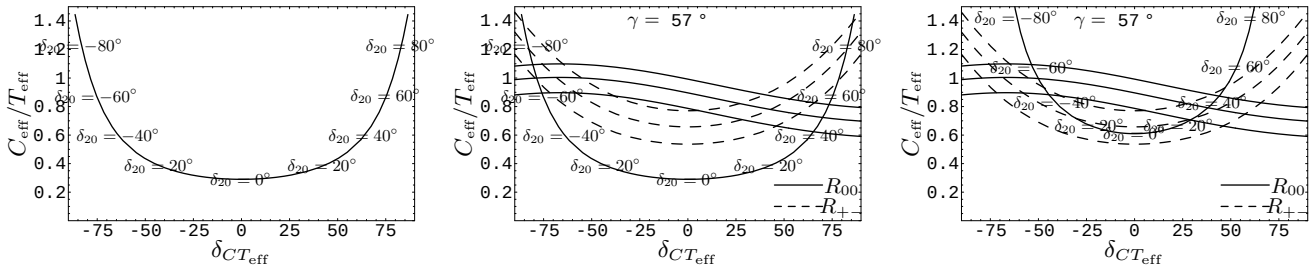

FIG. 3: The left figure is the plot of Eq. (43), the result including the FSI phase, in the plane of $\delta_{CT_{\rm eff}}$ (x-axis) versus $C_{\rm eff}/T_{\rm eff}$ (y-axis) by varying δ_{20}. The number on the line indicates the value of δ_{20} at each point. The bare value $C_0/T_0 = 0.29$ obtained from the default parameter sets of the QCD factorization with $\rho_{H,A} = 0$ is used. In the middle figure, we put together the left figure and the experimental bounds from R_{+-} and R_{00} for the case of $\gamma = 57^\circ$ (Fig.1 upper-right). The right figure is obtained in the same way as the middle one but using $C_0/T_0 \simeq 0.61$, the result with the parameter set called scenario 2 in QCD factorization.

$C_0/T_0 e^{i\delta_{CT_0}} \simeq 0.61 e^{-i3^\circ}$ for $\rho_{H,A} = 0$. Note that these lower value of λ_B and higher value of α_2^π must be carefully tested using other charmless B decays which often involve these two parameters. Fig. 2 (right most) shows the scattered plot produced as the other Fig 2 but with $\rho_A = 1$ and with parameter set of the scenario 2. We find $C/T \simeq 1.1$ can be achieved in this scenario if δ_{CT} is very small. Thus, QCD factorisation can solve the large C/T puzzle. Nevertheless, whether QCD factorisation can reproduce all the data in Eqs. (4) to (8) simultaneously depends not only on a large C/T but also its prediction on P/T and δ_{PT}, which must be carefully analysed by comparing e.g. to penguin dominant modes so as to make sure that our parameter sets are sensible.

IV. DOES FSI PHASE MAKE C/T LARGE?

In this section, we introduce the FSI phase into our QCD factorization analysis. In QCD factorization, this effect is ignored by arguing that the sum of the phases from all possible intermediate states cancel each other statistically. This argument has been challenged in, e.g. [34] where it is argued that this mechanism may work only in the inclusive processes and it is found that the strong phase in $B \to \pi\pi$ decays can be relatively large. Furthermore, it has been shown in [20] that the FSI phase can effectively enhance C/T, which is favoured by our analysis in section II. This is because of isospin invariance; the $B \to \pi^0\pi^0$ decay can be induced by the charge exchange scattering process $\pi^+\pi^- \to \pi^0\pi^0$ which effectively generates the C amplitude from T. Thus, we consider the case in which the QCD factorization amplitudes contain an additional large FSI phase between two isospin $I = 0, 2$ $B \to \pi\pi$ amplitudes, $\delta_{0,2}$, which can generate extra contributions to C of the QCD factorization computation. We examine whether the FSI effect can enhance sufficiently the value of C/T of the QCD factorization without adjusting the incalculable parameters $\rho_{H,A}$ and $\phi_{H,A}$ coming from the end-point singularities of the annihilation and hard scattering diagrams as shown in section III. For this purpose, we start from the QCD factorization amplitudes with $\rho_{A,H} = 0$ but with the FSI phase $\delta_{2,0}$ and evaluate C/T and furthermore constrain the values of δ_{20} and δ_{CT}. Note that we neglect inelastic FSI here. While comprehensive computations of the FSI phase can be found in [20] and [21] followed by [35] (and also in earlier ones [36] and [37]) where a large strong phase difference is found, we here examine these effects in a more phenomenological manner. In [38], a similar analysis with strong phases in the isospin amplitudes is performed and a large δ_{20} is found by a fit to the the central values of the experimental data. However, as we have seen in section II, the experimental errors are still large to constrain the phase δ_{CT} and consequently, the FSI phase, without a theoretical input.

Now, the effective parameters $T_{\rm eff}, C_{\rm eff}$, etc.. are related to the parameters in the previous section as

$$T_{\rm eff} e^{i\delta_{T_{\rm eff}}} = [(2T_0 - C_0)e^{i\delta_0} + (T_0 + C_0)e^{i\delta_2}]/3 \quad (40)$$

$$C_{\rm eff} e^{i\delta_{C_{\rm eff}}} = [-(2T_0 - C_0)e^{i\delta_0} + 2(T_0 + C_0)e^{i\delta_2}]/3 \quad (41)$$

$$P_{\rm eff} e^{i\delta_{P_{\rm eff}}} = P_0 e^{i(\delta_D + \delta_{0P})}. \quad (42)$$

For the parameters C_0, T_0, P_0 on the R.H.S., we use the QCD factorization prediction with $\rho_{H,A} = 0$ following our strategy mentioned above. Note that $P_{\rm eff}$ has not only the $I = 0$ phase, δ_{0P}, but also an extra phase, δ_D which may come from inelastic re-scattering, such as $DD \to \pi\pi$. As a result, the effective color-suppressed to color-allowed ratio is obtained as:

$$\left(\frac{C_{\rm eff}}{T_{\rm eff}}\right) e^{i\delta_{CT_{\rm eff}}} = \frac{(-2 + 2e^{i\delta_{20}}) + (1 + 2e^{i\delta_{20}})C_0/T_0}{(2 + e^{i\delta_{20}}) + (-1 + e^{i\delta_{20}})C_0/T_0} \quad (43)$$

The behaviour of this function with the value for C_0/T_0 in Eq. (38) is shown in Fig. 3 (left). We use the same $\delta_{CT_{\rm eff}}$ (x-axis) versus $(C/T)_{\rm eff}$ (y-axis) space shown in Fig. 1. The numbers on the line indicates the value of δ_{20} at each point. We can see that C/T indeed becomes larger as the FSI phase δ_{20} increases. We find e.g. that the bare ratio $C_0/T_0 = 0.29$ can be enhanced to $(C_{\rm eff}/T_{\rm eff}) \simeq 0.4$ for

$\delta_{20} \simeq \pm 21^\circ$, where $\delta_{CT_{\rm eff}} \simeq \pm 44^\circ$. In Fig. 3 (middle), we overlap Fig. 3 (left) and the experimental bounds for R_{+-} and R_{00} (Fig. 1 for $\gamma = 57^\circ$). We find that the allowed region from R_{+-} and R_{00} overlap at $\delta_{20} \simeq -65^\circ$, where $(C/T)_{\rm eff} \simeq 0.96$. Fig. 3 (right) is obtained in the same way as the middle figure but with using C_0/T_0 value from the scenario 2 in section III. We can find that the central value of (R_{+-}, R_{00}) are reproduced by $\delta_{20} \simeq 40^\circ$ where $C_{\rm eff}/T_{\rm eff} \simeq 0.8$ and $\delta_{CT_{\rm eff}} \simeq 40^\circ$.

In order to obtain a constraint on γ, we further need to know the maximum size of the FSI phase. For example, assuming $\delta_{20} \lesssim 30^\circ$, we find $\gamma \lesssim 48^\circ(55^\circ)$ using the default values for the input parameters of QCD factorization, i.e. using Eq. (38) and including $1\sigma(2\sigma)$ of the experimental errors in $S_{\pi^+\pi^-}, C_{\pi^+\pi^-}, R_{00}, R_{+-}$. However, as we have seen in Fig. 3, this result depends strongly on the inputs of QCD factorization. For example, with the scenario 2 of section III, we find that $\delta_{20} \lesssim 30^\circ$ leads to $\gamma = (59 \pm 3)^\circ (> 56^\circ)$. It is also important to mention that there may be a FSI contribution not only to the phase but also to C/T itself, as discussed in [35]. Therefore, the bound obtained here may receive a considerable corrections from both uncertainties of QCD factorization and of FSI. Further improvements in estimating those parameters are necessary for obtaining the bound for γ from this strategy.

V. CONCLUSIONS

We analysed the latest measurements of branching ratios and CP asymmetry in the $B \to \pi\pi$ processes and compared it to the theoretical model predictions. Using a model independent parameterisation of the $B \to \pi\pi$ process, we first constrained the penguin-tree ratio parameters, P/T and δ_{PT} by using the asymmetry measurements, $S_{\pi^+\pi^-}$ and $C_{\pi^+\pi^-}$ and then, using these values, we obtained the constraints for the color-suppressed and color-allowed tree ratio parameters, C/T and δ_{CT} for different given values of γ. We found that the errors in the branching ratios are still large and the allowed region for δ_{CT} is distributed in a quite large range. On the other hand, the value of C/T is found to be rather large for most of the parameter space and for example, we found $C/T \gtrsim 0.5$ for $\gamma > 47^\circ$.

Next, we examined whether this large value of C/T can be explained within the uncertainties of the theoretical model computations. We examined two theoretical models, i) QCD factorization varying $\rho_{H,A}$ and $\phi_{H,A}$ and ii) QCD factorization with $\rho_{H,A} = 0$ (no strong phase from perturbative part) but adding FSI phase. For i), we found that large $\rho_{H,A}$ lead to large values of C/T, especially when δ_{CT} is small. On the other hand, for ii), we found that C/T and δ_{CT} are enhanced when the FSI phase δ_{20} increases. As a result, we found that the large C/T can be explained in both cases, within the large theoretical uncertainties from meson distribution amplitudes, together with the end-point singularity for the former and with the FSI phase for the latter. We found that in general, the larger C/T can be realised for the smaller δ_{CT} for case i) and for the larger δ_{CT} for case ii). Therefore we will be able to distinguish these two sources of enhancement factors in near future by using the measurement of C_{00}. Namely, the ratio to C_{+-} yields

$$\frac{C_{00}}{C_{+-}} = \frac{C}{T}\frac{\sin(\delta_{CT} - \delta_{PT})}{\sin\delta_{PT}}\frac{1}{R_{00}}. \qquad (44)$$

One can see that typically, a small $\delta_{CT}(\simeq 0)$ leads to this ratio of order unity with negative sign, $C_{00}/C_{+-} \simeq -C/T/R_{00}$. For example, the central values of the experimental data for R_{00} and C_{+-} lead to $C_{00} = 0.57$ for $\delta_{CT} = 0$, which is close to the higher end of the current experimental value of C_{00} in Eq. (18). We can also see that a large $\delta_{CT}(\simeq \pm\pi/2)$ result shows a strong dependence on δ_{PT}, $C_{00}/C_{+-} \simeq \pm C/T/R_{00}/\tan\delta_{PT}$. Thus, for a more precise analysis, we will need a better knowledge about δ_{PT} from measurements of (S_{+-}, C_{+-}) as well as the prediction of δ_{PT} from each model. Note that the values of δ_{CT} and δ_{PT} are related in QCD factorisation through the parameters of the end-point singularity but are independent in FSI, especially due to a possible inelastic re-scattering phase δ_D of Eq. (42).

Acknowledgments

The work by E.K. was supported by the Belgian Federal Office for Scientific, Technical and Cultural Affairs through the Interuniversity Attraction Pole P5/27.

[1] P. Ball, S. Khalil and E. Kou, Phys. Rev. D **69** (2004) 115011 [arXiv:hep-ph/0311361].
[2] M. Gronau and J. L. Rosner, Phys. Rev. D **65** (2002) 093012 [arXiv:hep-ph/0202170].
[3] M. Gronau and J. L. Rosner, Phys. Rev. D **66** (2002) 053003 [Erratum-ibid. D **66** (2002) 119901] [arXiv:hep-ph/0205323].
[4] A. Ali, E. Lunghi and A. Y. Parkhomenko, Eur. Phys. J. C **36** (2004) 183 [arXiv:hep-ph/0403275].
[5] Y. Y. Charng and H. n. Li, Phys. Rev. D **71** (2005) 014036 [arXiv:hep-ph/0410005].
[6] P. Zenczykowski, Phys. Lett. B **590** (2004) 63 [arXiv:hep-ph/0402290].
[7] C. W. Chiang, M. Gronau, J. L. Rosner and D. A. Suprun, Phys. Rev. D **70** (2004) 034020 [arXiv:hep-ph/0404073].
[8] S. Mishima and T. Yoshikawa, Phys. Rev. D **70** (2004) 094024 [arXiv:hep-ph/0408090].

[9] X. G. He and B. H. J. McKellar, arXiv:hep-ph/0410098.

[10] M. Gronau, E. Lunghi and D. Wyler, Phys. Lett. B **606** (2005) 95 [arXiv:hep-ph/0410170].

[11] A. J. Buras, R. Fleischer, S. Recksiegel and F. Schwab, Acta Phys. Polon. B **36** (2005) 2015 [arXiv:hep-ph/0410407].

[12] Z. z. Xing and H. Zhang, Phys. Rev. D **71** (2005) 051302 [arXiv:hep-ph/0501016].

[13] M. Sowa and P. Zenczykowski, Phys. Rev. D **71** (2005) 114017 [arXiv:hep-ph/0502032].

[14] Y. Grossman, A. Hocker, Z. Ligeti and D. Pirjol, arXiv:hep-ph/0506228.

[15] M. Imbeault, arXiv:hep-ph/0505254.

[16] G. Raz, arXiv:hep-ph/0509125.

[17] M. Beneke, G. Buchalla, M. Neubert and C. T. Sachrajda, Nucl. Phys. B **591** (2000) 313 [arXiv:hep-ph/0006124].

[18] M. Beneke and M. Neubert, Nucl. Phys. B **675** (2003) 333 [arXiv:hep-ph/0308039].

[19] A. Khodjamirian, T. Mannel, M. Melcher and B. Melic, Phys. Rev. D **72** (2005) 094012 [arXiv:hep-ph/0509049].

[20] H. Y. Cheng, C. K. Chua and A. Soni, Phys. Rev. D **71** (2005) 014030 [arXiv:hep-ph/0409317].

[21] H. Y. Cheng, C. K. Chua and A. Soni, Phys. Rev. D **72** (2005) 014006 [arXiv:hep-ph/0502235].

[22] D. Chang, C. S. Chen, H. Hatanaka and C. S. Kim, arXiv:hep-ph/0510328.

[23] H. F. A. Group(HFAG), arXiv:hep-ex/0505100.

[24] A. J. Buras, R. Fleischer, S. Recksiegel and F. Schwab, Phys. Rev. Lett. **92** (2004) 101804 [arXiv:hep-ph/0312259].

[25] P. Ball and E. Kou, JHEP **0304** (2003) 029 [arXiv:hep-ph/0301135].

[26] V. M. Braun, D. Y. Ivanov and G. P. Korchemsky, Phys. Rev. D **69** (2004) 034014 [arXiv:hep-ph/0309330].

[27] S. J. Lee and M. Neubert, Phys. Rev. D **72** (2005) 094028 [arXiv:hep-ph/0509350].

[28] P. Ball and R. Zwicky, Phys. Lett. B **625** (2005) 225 [arXiv:hep-ph/0507076].

[29] C. W. Bauer, D. Pirjol, I. Z. Rothstein and I. W. Stewart, Phys. Rev. D **70** (2004) 054015 [arXiv:hep-ph/0401188].

[30] C. W. Bauer, D. Pirjol, I. Z. Rothstein and I. W. Stewart, arXiv:hep-ph/0502094.

[31] C. W. Bauer, I. Z. Rothstein and I. W. Stewart, arXiv:hep-ph/0510241.

[32] A. R. Williamson and J. Zupan, arXiv:hep-ph/0601214.

[33] M. Beneke and D. Yang, Nucl. Phys. B **736** (2006) 34 [arXiv:hep-ph/0508250].
M. Beneke and S. Jager, arXiv:hep-ph/0512351.

[34] M. Suzuki and L. Wolfenstein, Phys. Rev. D **60** (1999) 074019 [arXiv:hep-ph/9903477].

[35] S. Fajfer, T. N. Pham and A. Prapotnik Brdnik, Phys. Rev. D **72** (2005) 114001 [arXiv:hep-ph/0509085].

[36] J. M. Gerard, J. Pestieau and J. Weyers, Phys. Lett. B **436** (1998) 363 [arXiv:hep-ph/9803328].

[37] C. Isola and T. N. Pham, Phys. Rev. D **62** (2000) 094002 [arXiv:hep-ph/9911534].

[38] L. Wolfenstein and F. Wu, Phys. Rev. D **72** (2005) 077501 [arXiv:hep-ph/0506224].